Electronic Supplementary Material (ESI) for Analyst

ELECTRONIC SUPPLEMENTARY

INFORMATION FOR:

One-Step Assay for Influenza Virus Using Dynamic Light Scattering and Gold Nanoparticle Labels

Jeremy D. Driskell[*]*, Cheryl A. Jones, S. Mark Tompkins, and Ralph A. Tripp*

University of Georgia, Department of Infectious Diseases, Nanoscale Science and Engineering Center, Athens, GA 30602

EXPERIMENTAL METHODS

Characterization of Antibody Specificity. The specificity and cross-reactivity of mAb clone IC5-4F8 for whole influenza viruses was evaluated via ELISA and microneutralization assays. Briefly, viral stocks were diluted with PBS to a concentration of 5.62 x 10^5 $TCID_{50}$/mL to perform the ELISA. Virus or naïve allantoic fluid (100 μL) was then added to each well of an Immulon 2-HB 96-well flat bottom microtiter plate (Thermo Scientific, Rochester, NY) and allowed to incubate overnight at 4 ˚C to allow adsorption of virus to the plates. The plates were then thoroughly rinsed with KPL wash buffer (2mM imidazole buffered saline, 0.02% Tween 20; Gaithersburg, MD) and blocked with 100 μL/well blocking buffer (PBS containing 0.5% BSA and 5% non-fat dry milk) for 1 hour at room temperature. Two-fold serial dilutions of mAb NR-4542 (100 μL/well), starting with a 1:500 dilution, were added to the pre-adsorbed wells for 1 hour at room temperature. HRP-labeled goat anti-mouse IgG (H+L) (Thermo Scientific, Rockford, IL) served as the secondary antibody to bind mAb NR-4542. 3,3',5,5'-Tetramethylbenzidine (TMB, Vector Laboratories, Burlingame, CA) was added as a substrate and the absorbance of the enzymatic product was read out at 450 nm using a plate reader (BioTek, Winooski, VT) to quantify the interaction of mAb NR-4542 with whole influenza virus.

The microneutralization assay was adapted from a previously described procedure.[1] Two-fold dilutions of mAb NR-4542 were prepared using infection media (MEM+L-glut+1% antibiotics/antimycotics) in a 96-well round-bottom plate (Corning, Corning, NY), starting with 5 μg per well. Influenza virus was added to the diluted mAb at 100 $TCID_{50}$/well and incubated at 37 ˚C with 5% CO_2 for 1 hour to allow the mAb to bind to the virus. Control wells of virus plus infection media and infection media only were included on each plate. The mAb/virus mixture was then transferred to corresponding wells of a previously prepared 96-well flat-bottom tissue

culture plate with a 90% confluent monolayer of MDCK cells. Following 72 hours of incubation at 37 ˚C with 5% CO_2, viral replication was detected via hemagglutination of chicken red blood cells.

Preparation and Characterization of Antibody-modified AuNPs. Borate buffer (50 mM, 40 μL, pH 8.9) was added to a 1.0-mL suspension of 60-nm AuNP to adjust the pH. This basic pH facilitates the reaction between the mAb and the cross linking agent in subsequent steps and provides greater resistance to AuNP aggregation. Next, 10 μL of 1 mM DTSSP was added to the AuNPs and mixed for 30 minutes. In this step, DTSSP adsorbs onto AuNPs to form a thiolate moloayer through cleavage of the disulfide bond yielding a terminal succinimidyl ester. The suspension was then centrifuged at 7000g for 5 minutes. The supernatant containing excess DTSSP was decanted and the AuNPs were resuspended in 2 mM borate buffer (pH 8.9). Monoclonal antibody (20 μg) was added to the AuNPs and allowed to react for 1.5 hours. During this step, deprotonated primary amines of the antibody couple to the succinimidyl ester to form an amide linkage.[2] The suspension was then centrifuged at 7000g for 5 minutes, the supernatant was decanted, and the AuNP was resuspended in 2 mM borate buffer (pH 8.9) containing 1% BSA. The centrifugation/resuspension cycle was repeated one additional time for thorough removal of excess mAb. The suspension was aged for 30 minutes to allow the BSA to block any unreacted DTSSP and nonspecific binding sites. A small volume of concentrated solution of NaCl (10%) was added to the suspension to yield a final NaCl concentration of 150 mM prior to use in an immunoassay in order to mimic physiological conditions. The electrolyte is essential for the antibody to maintain proper 3-dimensional structure and thus, binding capacity to the target antigen.

RESULTS AND DISCUSSION

Antibody Reactivity. An ELISA for mAb clone IC5-4F8 was performed against several strains of influenza using the whole virus as the antigen adsorbed onto the microtiter plate as shown in Figure S-1 (Supporting Information). mAb clone IC5-4F8 bound PR8 diluted to 1:2000, and showed no cross reactivity with A/New Caledonia/20/99 (H1N1; New Caledonia) or A/swine/Minnesota/ 02719/2009 (H3N2; MN02719) influenza A viruses. These data demonstrate the high specificity of mAb clone IC5-4F8 for PR8. However, as adsorption of the virus to a microtiter plate may alter its native three-dimensional structure further testing was done to establish its ability to bind whole virus under soluble conditions, e.g., in solution, in which the DLS assay is to be conducted. Therefore, a microneutralization assay was performed to evaluate mAb-virus binding in solution. In a microneutralization assay virus is incubated with dilutions of the mAb in solution prior to addition to susceptible cells (e.g. MDCK cells) that allow for viral replication. Binding of the mAb to the virus HA prevents viral attachment to the cell membrane and inhibits viral replication. mAb clone IC5-4F8 was confirmed in this study to bind and neutralize PR8 requiring a minimum of 156 μg of mAb per 100 $TCID_{50}$ (data not shown).

AuNP-Antibody Conjugation. It is important to maximize antibody coupling to AuNP as the sensitivity of the assay is correlated to the coupling efficiency. A greater number of antibodies per AuNP provides more binding sites for the target influenza shifting equilibrium toward the Ag-Ab complex and will yield more extensive influenza-induced AuNP aggregation. Antibody coating of the AuNP is also essential for particle stability. Citrate capped AuNP are susceptible to aggregation in electrolytic (>10 mM) solutions, such as biological matrices (~150 mM NaCl). However, it is well established that conjugation of AuNPs with a protein layer, such as an antibody, protects the particles from aggregation even in highly electrolytic environments.[3, 4]

Effective conjugation of the antibody to the AuNP is dependent upon the antibody concentration and solution pH during the modification step, and must be optimized for each protein as demonstrated below. It should be noted that we utilized the bifunctional cross linking agent, DTSSP, to covalently conjugate the antibody to the AuNP, in an attempt to improve the integrity of the reagent relative to physisorption by reducing antibody desorption.[5] In the event of desorption, free antibody would compete with AuNP-conjugated antibody for influenza binding sites and result in decreased assay performance.

Flocculation tests were performed in which varying amounts of mAb clone IC5-4F8 were added to 60 nm AuNP at pH 6.9, 7.9, and 8.9 and nanoparticle aggregation was monitored upon addition of 150 mM NaCl via UV-visible spectrophotometry.[4] Extinction spectra for experiments carried out at pH 8.9 are displayed in Figure S-2. As anticipated, the surface plasmon resonance band, λ_{max}, is red-shifted and broadened, indicating AuNP aggregation, for low concentrations of mAb (<20 μg/mL). At higher concentrations of mAb, e.g., 20 and 40 μg/mL, a sufficient number of protein molecules are available for complete protection of the AuNP and the shift in λ_{max} is negligible. Moreover, the ratio of A_{700nm} to A_{532nm}, an experimental parameter to quantify aggregation,[6-8] is constant for mAb concentrations greater than 20 μg/mL at pH 8.9 (Figure S-3). The results for antibody-AuNP conjugation at pH 6.9 and 7.9 are also shown in Figure S-3. It was determined that mAb clone IC5-4F8 does not fully stabilize AuNP at pH 6.9 and that higher concentrations of antibody are required to fully coat the AuNP at pH 7.9. These findings are consistent with previous reports that suggest a pH slightly basic of the protein pI (~0.5 pH units) is optimal for conjugation to AuNP.[3] These data demonstrate that a minimum of 20 μg mAb clone IC5-4F8 is required to fully label 1.0 mL of AuNP (2.6×10^{10} particles/mL) at pH 8.9.

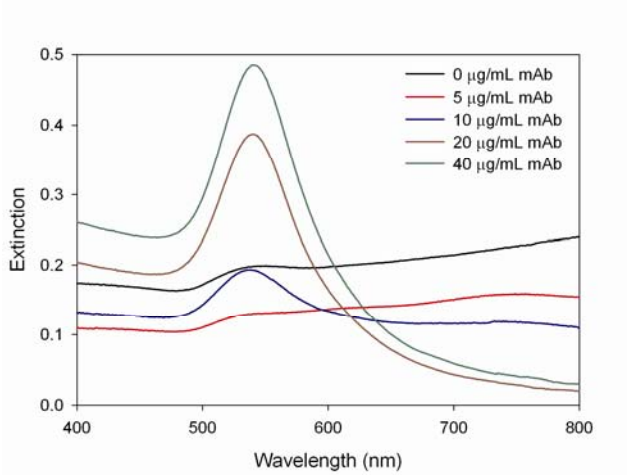

Fig. S-1. UV-visible extinction spectra of 1 mL AuNPs (60 nm) after mixing with mAb clone IC5-4F8 (0-40 μg) for 1 h, followed by the addition of 150 mM NaCl.

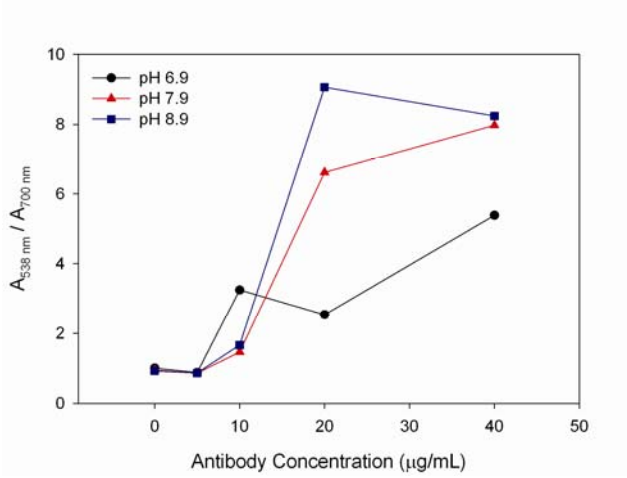

Fig. S-2. UV-visible extinction spectra of 1 mL AuNPs (60 nm) after mixing with mAb clone IC5-4F8 (20 μg) at pH 6.9, 7.9, and 8.9 for 1 h, followed by the addition of 150 mM NaCl.

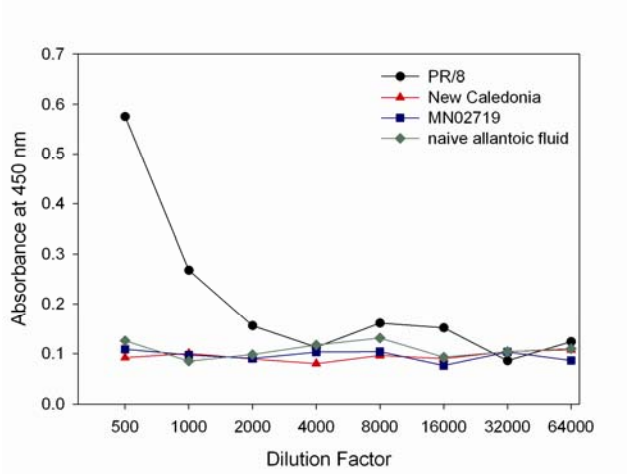

Fig. S-3. ELISA results for the binding of mAb clone IC5-4F8 to influenza A virus strains PR/8, New Caledonia, and MN 02719. Naïve, uninfected allantoic fluid served as a negative control.

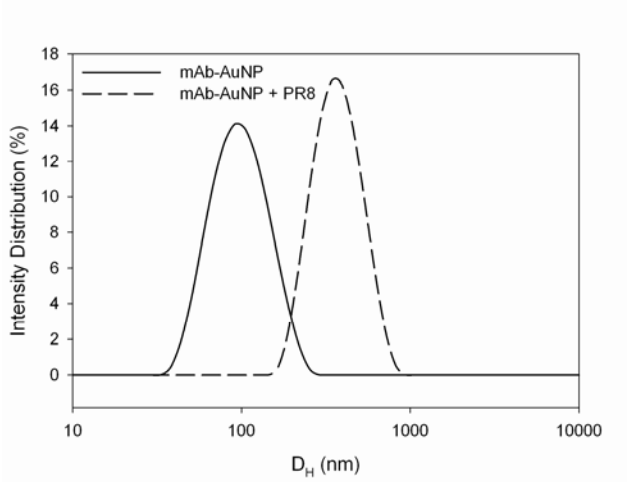

Fig. S-4. DLS determined particle size distribution for the AuNP probes before and after the addition of influenza virus. The size distribution was calculated based on the scattering intensity.

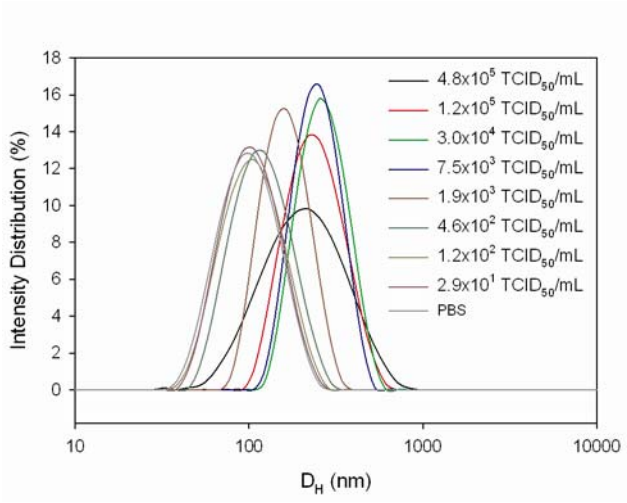

Fig. S-5. DLS determined particle size distribution curves for the calibration curve plotted in Figure 2 of the manuscript. The size distribution was calculated based on the scattering intensity.

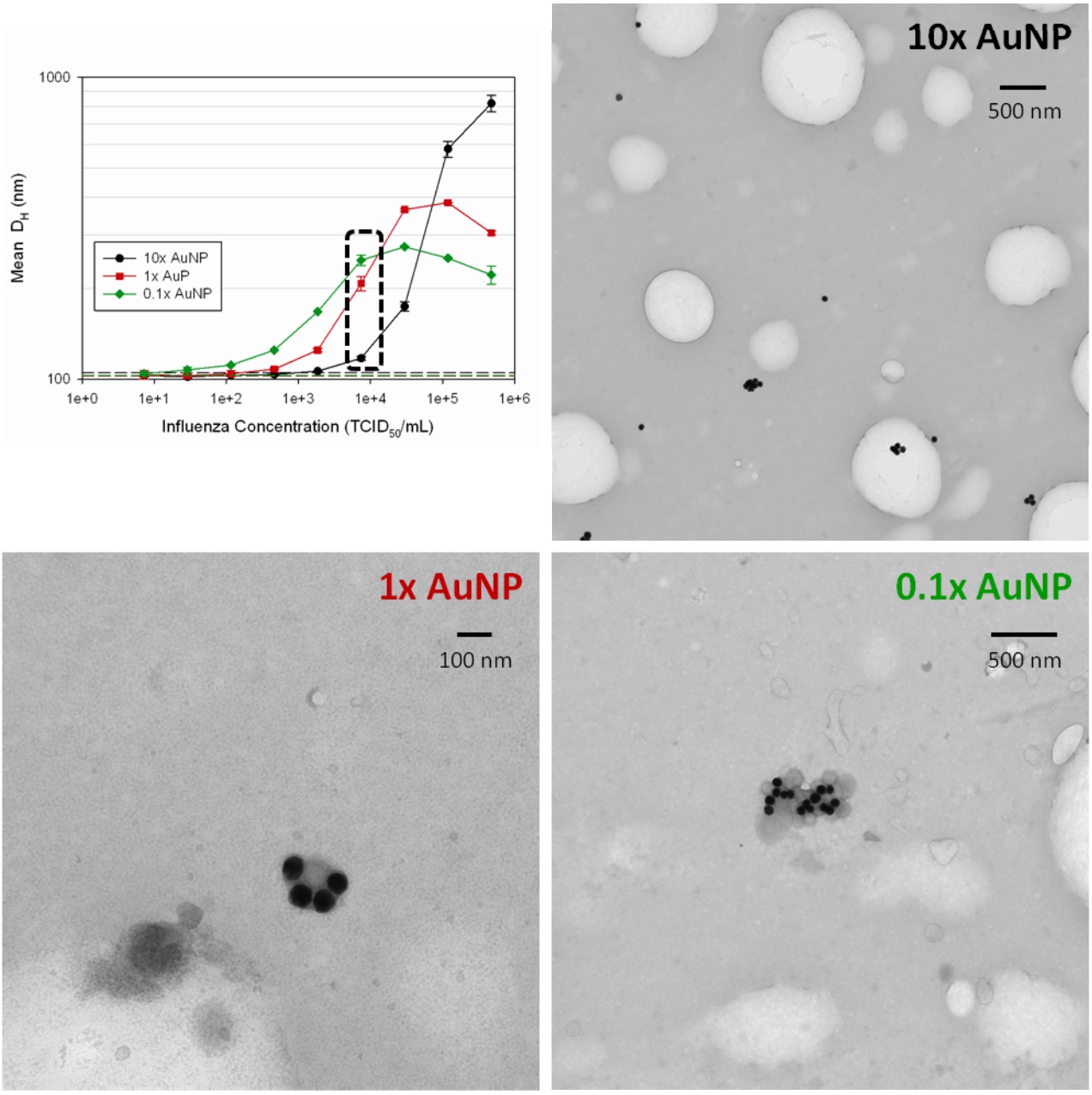

Fig. S-6. DLS calibration curves as an effect of AuNP probe concentration and TEM micrographs corresponding to highlighted data points (dashed rectangle). The TEM images suggest that more extensive aggregation occurs at the hook point and that as the concentration approaches the detection limit, the viruses are ”encapsulated” by the AuNP probe With excess probe in solution. Note the abundance of single AuNP probes in the 10x AuNP image. After surveying the entire TEM grid for the 1x AuNP sample, no excess single AuNP probes could be found.

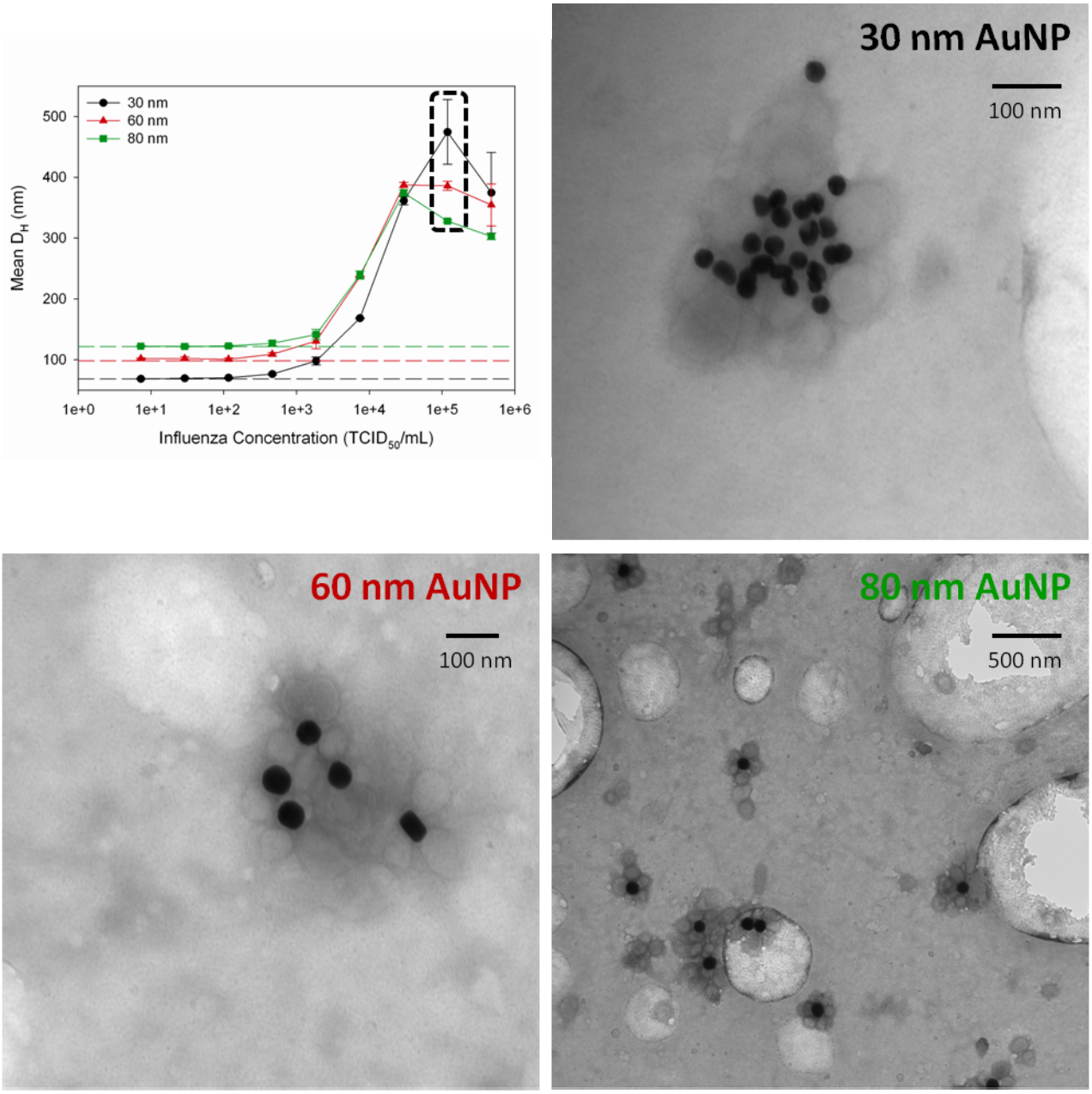

Fig. S-7. DLS calibration curves as an effect of AuNP probe size and TEM micrographs corresponding to highlighted data points (dashed rectangle). The TEM images suggest that more extensive aggregation occurs at the hook point and that at concentrations above the hook point the binding sites on the AuNP probe becomes saturated with virus to result in a decreased mean hydrodynamic diameter.

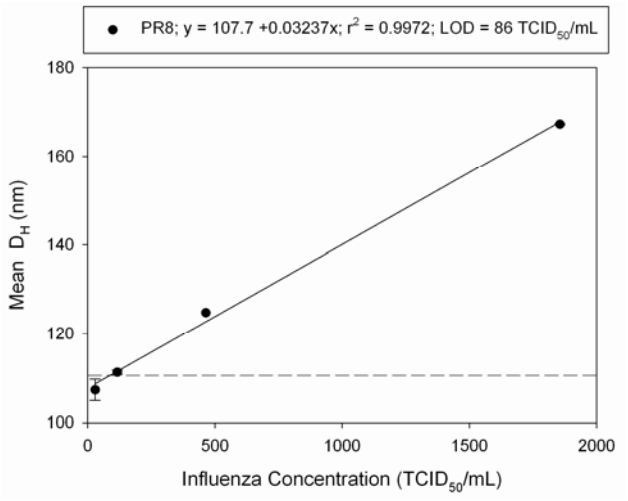

Fig. S-8. DLS calibration curve plotted on a linear scale for the low concentration data presented in Fig. 2A. The data are best fit to a linear function (solid line) and the horizontal dashed line represents the minimum detectable signal that is defined as the PBS blank signal plus three times its standard deviation.

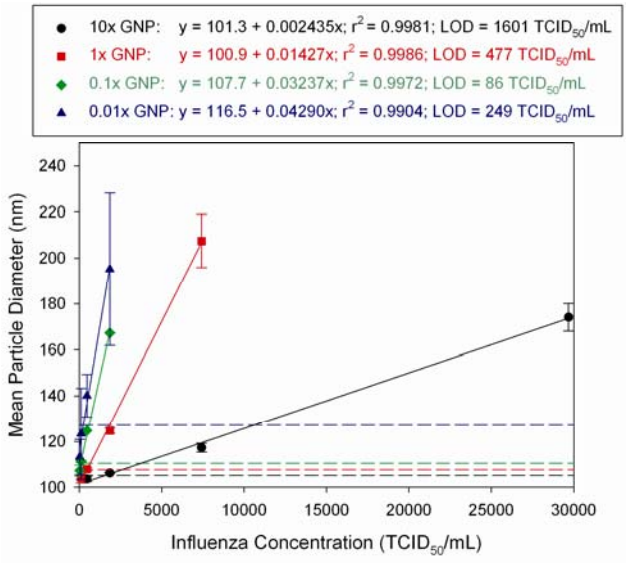

Fig. S-9. DLS calibration curves plotted on a linear scale for the low concentration data presented in Fig. 3. The data are best fit to a linear function (solid lines) and the horizontal dashed lines represent the minimum detectable signal that is defined as the PBS blank signal plus three times its standard deviation.

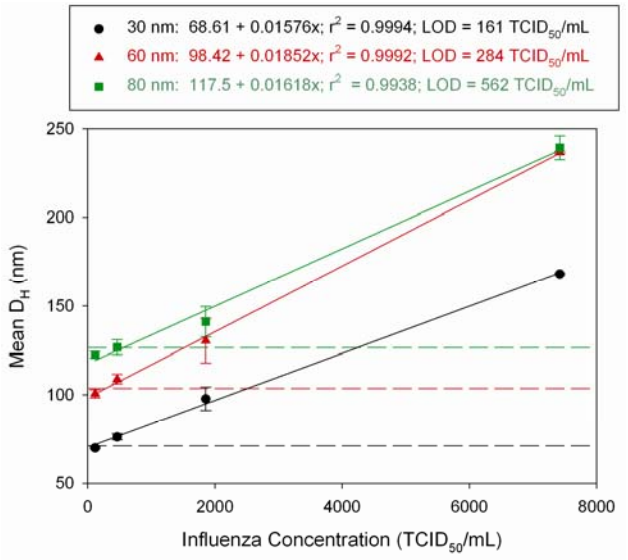

Fig. S-10. DLS calibration curves plotted on a linear scale for the low concentration data presented in Fig. 4. The data are best fit to a linear function (solid lines) and the horizontal dashed lines represent the minimum detectable signal that is defined as the PBS blank signal plus three times its standard deviation.

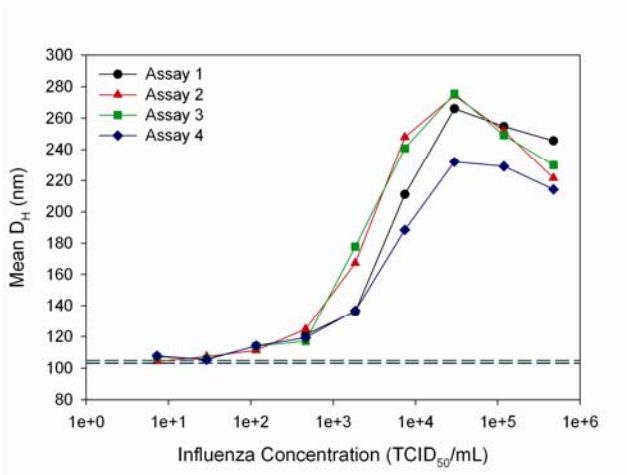

Figure S-11. Reproducibility of DLS calibration curve for influenza virus assay. The assays were performed over a period of several months using independently prepared samples and AuNP probes.

REFERENCES

1. Rowe, T., Abernathy, R. A., Hu-Primmer, J., Thompson, W. W., Lu, X. H., Lim, W., Fukuda, K., Cox, N. J., Katz, J. M. *J. Clin. Microbiol.* **1999**, *37*. 937-943.
2. Wagner, P., Hegner, M., Kernen, P., Zaugg, F., Semenza, G. *Biophys. J.* **1996**, *70*. 2052-2066.
3. Beesley, J. E., *Colloidal Gold: A New Perspective for Cytochemical Marking*. Oxford Universitiy Press: Oxford, U.K., 1989; Vol. 17.
4. Geoghegan, W. D., Ackerman, G. A. *J. Histochem. Cytochem.* **1977**, *25*. 1187-1200.
5. Ni, J., Lipert, R. J., Dawson, G. B., Porter, M. D. *Anal. Chem.* **1999**, *71*. 4903-4908.
6. Ou, L. J., Jin, P. Y., Chu, X., Jiang, J. H., Yu, R. Q. *Anal. Chem.* **2010**, *82*. 6015-6024.
7. Su, X. D., Kanjanawarut, R. *Acs Nano* **2009**, *3*. 2751-2759.
8. Weisbecker, C. S., Merritt, M. V., Whitesides, G. M. *Langmuir* **1996**, *12*. 3763-3772.